

Chapter 2

Introduction to Biopotential Acquisition

2.1 Introduction

The biopotential readout circuits have to cope with various problems, while extracting the biopotential signals from the human body. These problems are not only due to the extremely weak characteristics of the biopotential signals but also due to the environment and the apparatus that are being used during the signal acquisition. Therefore, the design of a readout circuit for the biopotential acquisition systems requires a solid understanding of not only the analog circuit design techniques but also the origin and the characteristics of the biopotential signals.

This Chapter gives a brief introduction to the challenges of extracting biopotential signals. Section 2.2 introduces the genesis of the biopotential signals, and presents the frequency and the amplitude characteristics of the EEG, ECG, and EMG signals. Section 2.3 explains the chemistry of the biopotential electrodes, which acts as a transducer between the human body and the readout circuit, and describes the non-ideal characteristics of the biopotential electrodes. Section 2.4 introduces the interference theory, i.e. the theory of the common-mode interference from the mains. This Section also presents the state-of-the-art in IA design, the building block that defines the quality of the extracted signals from the biopotential electrodes. Section 2.5 describes the chopper modulation technique, which is used in the literature to achieve low-noise and high-CMRR IAs. Finally, Sect. 2.6 states the conclusions of this Chapter.

2.2 Introduction to Biopotential Signals

Biopotential signals are generated due to the electrochemical activity of certain class of cells that are components of the nervous, muscular or glandular tissue. Electrically, these cells exhibit a resting potential, and when they are stimulated they generate an action potential. The electrical activity of each cell is described by the ion exchange through the cell membrane. The membrane potential of an inactive cell is called the *resting potential*. At the rest state, the membrane of the cell is more permeable to K^+ than Na^+ , and K^+ concentration of the interior of the cell is much higher than the exterior. Therefore, a diffusion gradient of K^+ occurs towards the exterior of the cell making the interior more negative relative to the exterior, which results in an electrical field build up towards the interior of the cell. At steady state, the diffusion gradient of the K^+ ions are balanced by the electrical field and the equilibrium is reached with a polarization voltage of nearly -70 mV. When the cell is electrically stimulated (through the central nervous system), the permeability of

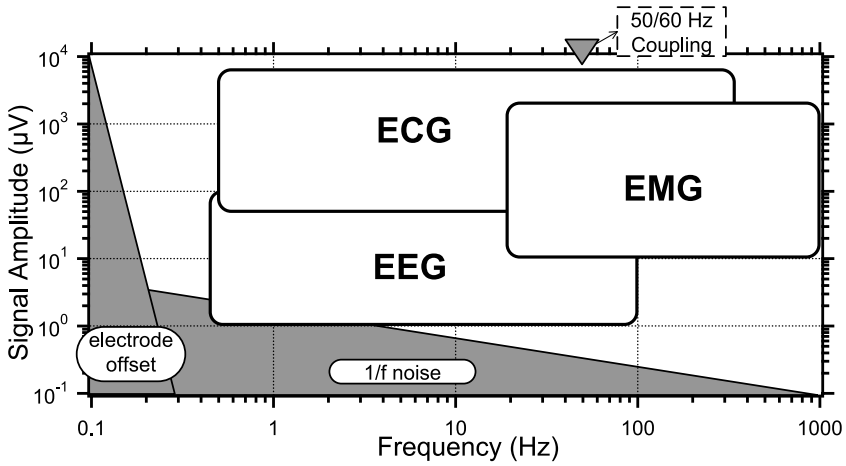


Fig. 2.1 Frequency and amplitude characteristics of the biopotential signals, EEG, ECG, and EMG, and the correlating signals of the biopotential signals

the membrane to Na^+ ions increases. Thus, Na^+ ions diffuse toward the inside of the cell, resulting in a potential increase of the interior of the cell. As the potential reaches to +40 mV, the permeability of the membrane to Na^+ ions decreases and to K^+ increases, resulting in a sharp decrease in the membrane potential towards its rest state. This cycle of the cellular potential is called the action potential, and the biopotential signals, such as EEG, ECG, EMG, are the result of several action potentials produced by a combination of different cells [11].

EEG is the measure of the electrical activity of the brain created by a group of neurons. Electrodes are placed on the predefined locations of the scalp [12], and the voltage of the electrodes versus a reference is measured. Similarly, ECG is the measure of the electrical activity of the heart. It is extracted from the electrodes on the chest, and it is characterized by its three main features, the P-wave, the QRS-complex, and the T-wave [11]. Finally, EMG is the electrical potential of the skeletal muscle cells, which is generated during the contraction of the muscle.

Figure 2.1 shows the frequency and amplitude characteristics of EEG, ECG, and EMG waves, when recorded by surface electrodes [11]. In order to extract the biopotential signals, the correlating signals, such as the $1/f$ noise of the CMOS transistors, the interference from the mains, and the DC differential electrode offset voltage between the biopotential electrodes, must be rejected or filtered by the readout circuit.

2.3 Introduction to Biopotential Electrodes

Although readout circuits implemented in CMOS technology usually have very large input impedance, a non-zero current should flow from the body to the input

of the readout circuit. However, this current is carried by ions in the body, whereas it is carried by electrons on the wires connecting the electrodes to the readout circuit. Therefore, a transducer interface is necessary between the body and the readout circuit that converts the ionic current into electronic current, or vice versa. This interface is called a biopotential electrode.

The operation principle of a biopotential electrode can be described by an electrode–electrolyte interface. In order to allow the current flow between the electrolyte, which has no free electrons, and the electrode, which has no free cations or anions, a chemical reaction has to occur at the interface that can be represented by the following general equations:



In this equation, C and A stands for the cations and anions in the electrolyte, respectively, and it has been assumed that the electrode is made up of the cations of the electrolyte. Therefore, the cations in the electrode can oxidize at the interface, and the anions coming to the interface can be oxidized to a neutral atom, both resulting in a free electron in the electrode. Thus, current can pass from the electrode to the electrolyte. Similarly, the reduction reactions create current in the reverse direction.

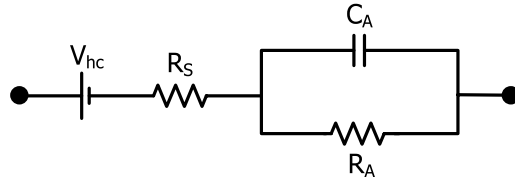
Therefore, if a metal is inserted in a solution, which has the ions of the same metal and some anions to preserve the neutrality of the solution, the reactions given in (2.1) starts to occur depending on the concentration of the cations in the solution. This disturbs the neutrality of the solution, and a charge gradient builds up at the electrode–electrolyte interface, resulting in a potential difference that is called the *half-cell potential*. The mismatch of the half-cell potential between the reference electrode and the recording electrode is responsible for the differential DC electrode offset voltage.

2.3.1 Equivalent Circuit Model

Biopotential electrodes can be grouped as, *polarizable* and *non-polarizable* electrodes. The perfectly polarizable electrodes have no actual charge transfer between the electrode–electrolyte interface. Thus, such electrodes behave as capacitors and the current is due to the displacement current. On the other hand, the current passes freely across the electrode–electrolyte interface of the non-polarizable electrodes, thus these electrodes behave as a resistor. However, neither of the two types can be fabricated. Thus, practical electrodes are somewhere in between these two types.

The equivalent circuit of an electrode can be described as shown in Fig. 2.2. C_A and R_A represents the impedance associated with the electrode–electrolyte interface, and R_S is the resistance of the electrolyte solution. The half-cell potential of the interface is represented with a voltage source, V_{hc} .

Fig. 2.2 Equivalent circuit model of a biopotential electrode



In conventional electrodes, the electrolyte represents the gel that is used in between the tissue and the electrode. Since the biopotential signals are generally extracted differentially from two electrodes, there is always a mismatch between the half-cell potentials due to the difference in the gel–tissue interface (sweat glands and different epidermis effect the half-cell potentials of the electrodes [11]). Therefore, there appears a DC potential between the two electrodes, which is much larger than the μV level biopotential signals. This DC potential will be referred as differential DC electrode offset voltage in the rest of the text. Hence, the biopotential readout circuit should exhibit high-pass filter (HPF) characteristics to prevent the saturation of the readout circuit.

2.3.2 Types of Biopotential Electrodes

Biopotential electrodes can also be classified as: wet, dry, and non-contact electrodes. Wet electrodes use a gel type electrolyte between the electrode and the surface of the skin. The most common type of a wet electrode is the Ag/AgCl electrode. Its characteristic approaches that of a perfectly non-polarizable electrode. The electrode metal is made up of Ag, which is coated with an AgCl layer. An electrolyte gel is used to establish the electrical contact between the electrode and the surface of the skin. The most important advantages of the Ag/AgCl electrodes are their low impedance and low artifact due to the motion of artifact. On the other hand, the use of the gel creates discomfort and increases the preparation time of the acquisition system.

Dry electrodes, as their name imply, do not use any kind of gel to make contact between the electrode and the body. Thus, they are more comfortable and easy to prepare compared to the wet electrodes. However, due to the lack of the electrolyte, their characteristics are closer to a polarizable electrode, which can be characterized as a leaky capacitor. Therefore, the readout circuit for a dry electrode must have very high input impedance ($\gg 1\text{ G}\Omega$). Moreover, due to the very high impedance, the readout circuit must be placed very close to the electrode in order to prevent the electromagnetic interference. This can be achieved by using active electrodes [13]. However, the main disadvantage of the active electrodes is the necessity for matched components to achieve high CMRR, which is not straight forward in CMOS process. Alternatively, the characteristics of the dry electrodes can be improved by utilizing the advantages of MEMS processing technology to prevent the active electrode usage. Reference [14] proposes a dry electrode with micromachined spikes, where

these spikes can penetrate through the stratum corneum of the skin, and bring the electrode directly in contact with the electrically conductive living epidermis. Test results shows that this dry electrode achieves $87\text{ k}\Omega$ at 0.6 Hz , and the arithmetic mean of the offset voltage between two electrodes is 11.8 mV , which is comparable to the performance of wet electrodes.

Non-contact electrodes can be considered as a pure capacitor between the human body and the readout electronics, so they allow remote sensing of the biopotential signals [15]. They are intrinsically safe (no DC current drawn from the body) and biocompatible. However, the input impedance of the readout circuit must be extremely high for extracting the biopotential signals from non-contact electrodes. In addition, any motion of the electrode with respect to the body will create an artifact due to the change of capacitance. References [16] and [17] demonstrate ECG and EEG signals using non-contact electrodes.

2.4 Introduction to Biopotential Amplifiers

The essential purpose of a biopotential amplifier is to amplify and filter the extremely weak biopotential signals. However, the design of this amplifier is not straight forward. Biopotential amplifiers must cope with various challenges in order to extract the biopotential signals. Meanwhile, the power dissipation of the amplifier must be minimized for long-term power autonomy. The challenges of designing a biopotential amplifier for portable biopotential acquisition systems can be summarized as follows:

- High CMRR to reject interference from mains.
- HPF characteristics for filtering differential DC electrode offset.
- Low-noise for high signal quality.
- Ultra-low power dissipation for long-term power autonomy.
- Configurable gain and filter characteristics that suit the needs of different biopotential signals and different applications.

Figure 2.1 shows the frequency characteristics of the correlating signals for the biopotential signals. The interference from the mains to the human body appears at the $50/60\text{ Hz}$ and at its harmonics. Thus, amplifier must have high CMRR in order to reject this common-mode signal. The differential DC electrode offset voltage, which is orders of magnitude larger than the biopotential signals, must be rejected to prevent the saturation of the amplifier. Therefore, the biopotential amplifier must have HPF characteristics. Meanwhile, the biopotential amplifier should minimize its power dissipation to improve the power autonomy. Subsection 2.4.1 will describe the theory of interference from the mains, and Sect. 2.4.2 will describe a parameter called NEF that can be used to compare the power-noise performance of the different amplifiers.

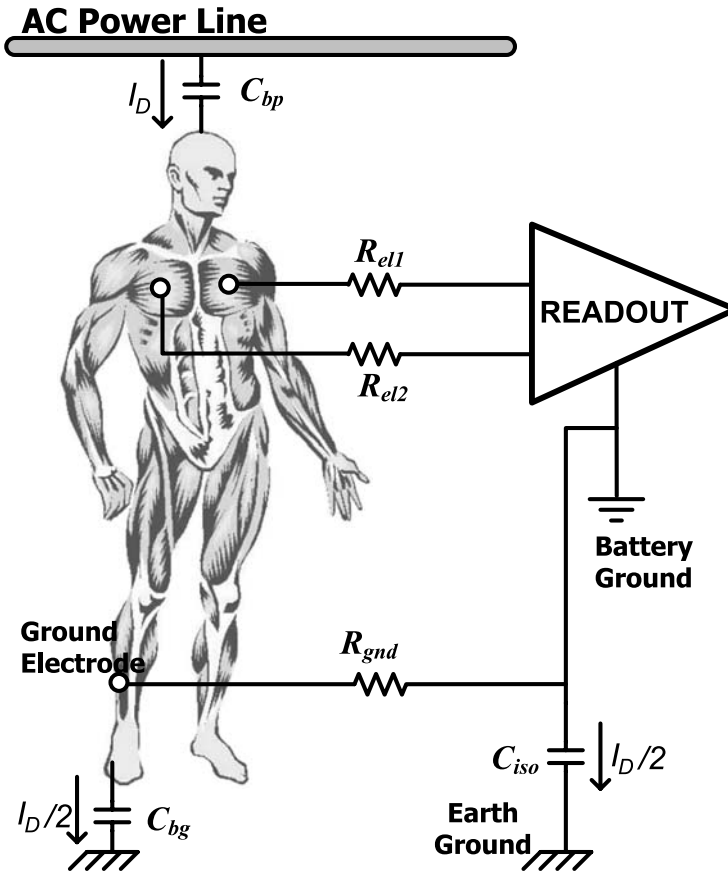


Fig. 2.3 Electrostatic interference to the human body

2.4.1 Interference Theory

Biopotential acquisition systems are often disturbed by the interference from the mains. Two main types of interference are called the electromagnetic interference and the electrostatic interference. In the case of the electromagnetic interference, the magnetic field created by the alternating mains current cuts the loop enclosed by the human body, the leads of the circuit, and the biopotential amplifier. This induces an electromotive force (EMF), which creates an AC potential at the input of the circuit. The electromagnetic interference can be reduced by decreasing the area of the loop by twisting the cables [18]. Further reduction is possible by using miniaturized portable biomedical acquisition systems that can be placed much closer to the electrodes, which in turn reduces the cable length.

Figure 2.3 shows the equivalent circuit for describing the electrostatic interference [10]. The human body is capacitively coupled to the mains via C_{bp} and also to the ground via C_{bg} . In addition to these two capacitances, there exists an isolation

capacitance between the earth and the ground of the amplifier battery. As a result, the path through the coupling capacitors creates a displacement current, I_D , passing through the human body and splitting equally between the C_{bg} and C_{iso} [19] (C_{bg} and C_{iso} have similar capacitance values and R_{gnd} is much smaller than the impedance of C_{iso} and C_{bg} at 50 Hz/60 Hz). Therefore, an AC voltage with magnitude:

$$V_{CM} = \left(\frac{I_D}{2} \right) R_{gnd} \quad (2.2)$$

is created on the human body. Unless there is a mismatch between R_{el1} and R_{el2} , this voltage appears as a common-mode input to the amplifier, and can be rejected by the amplifiers high CMRR. However, there is always a mismatch between the electrode impedances, due to this mismatch, a differential error signal is created with amplitude:

$$\Delta V_{IN} = V_{CM} \left(\frac{|R_{el1} - R_{el2}|}{Z_{in}} \right) \quad (2.3)$$

where Z_{in} stands for the input impedance of the amplifier [18]. As a conclusion, a high CMRR alone is not sufficient for an IA to completely reject the electrostatic interference. In addition, it should implement very high input impedance.

2.4.2 Noise-Efficiency Factor (NEF) of Biopotential Amplifiers

Due to the small frequency bandwidth of the biopotential signals, it is the target noise level that defines the power dissipation of the biopotential amplifiers. As the type and the number of noise sources increase, the total noise of the amplifier also increases. Therefore, the amplifier requires more power to achieve the target noise level. The term called *noise-efficiency factor* (NEF) is first introduced by [20] in order to compare the power–noise performance of different amplifiers and can be expressed as:

$$NEF = V_{in,rms} \sqrt{\frac{2I_{tot}}{\pi V_t 4kTBW}} \quad (2.4)$$

where BW is the -3 dB bandwidth of the amplifier and $V_{in,rms}$ is the total input referred voltage noise of the amplifier. The NEF of a single bipolar transistor having only thermal noise is 1, which is the theoretical limit for any practical circuit. NEF can be used to compare the power–noise performance of different amplifiers. The amplifier with lower NEF can achieve lower power dissipation for a given noise level.

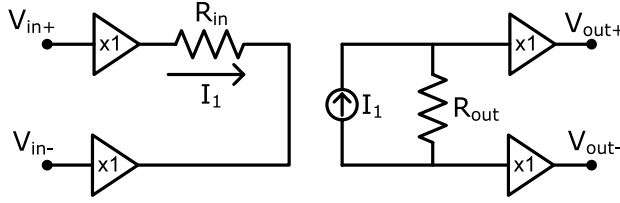


Fig. 2.4 Simplified schematic of a current balancing IA

2.4.3 State-of-the-Art in Instrumentation Amplifier Design

The IA is the most critical building block of the analog readout front-end in terms of the signal quality and clarity. It defines the noise level and the CMRR of the readout front-end, and filters the differential DC electrode offset. Hence, it is generally the most power consuming building block of an analog readout front-end. Therefore, the design effort focuses on implementing a low-power and low-noise IA.

The most common and well-known IA architecture is called the three-opamp architecture [21–25]. However, it is very-well known that the CMRR of the three-opamp IA is highly dependent on the matching of the resistors [26]. This matching requires laser trimming in standard CMOS technology that increases the cost. In addition to that, the necessity for low output impedance opamps for driving the feedback resistors, results in excessive power dissipation.

A second technique for implementing IAs uses switched-capacitor (SC) architectures [27, 28]. Although SC amplifiers are capable of eliminating the $1/f$ noise of the CMOS transistors, they suffer from the noise fold-over above Nyquist frequency (half of the sampling frequency) [29]. In order to compensate this increase in noise, the power dissipation of the SC amplifiers has to be increased. Therefore, SC architectures are not efficient for low-power and low-noise IAs.

Another IA topology is called Current Balancing (Current Feedback) IA (CBIA) [20, 30–33]. Figure 2.4 shows the simplified block diagram of a CBIA. The input stage acts as a transconductance amplifier. The current passing through R_{in} is copied to the transresistance stage, and the voltage created on R_{out} is buffered to the output. Therefore, the voltage gain of the CBIA can be written as:

$$(V_{out+} - V_{out-}) = \frac{R_{out}}{R_{in}} (V_{in+} - V_{in-}) \quad (2.5)$$

where the ratio of the two resistors defines the voltage gain of the CBIA. Thus, the CBIA topology eliminates not only the need for matched resistors for achieving high CMRR but also the need for low output impedance amplifiers. Therefore, the CBIA topology is convenient for implementing low-power and low-noise IAs. Table 2.1 summarizes the properties of three-opamp, switched-capacitor, and CBIA architectures for biopotential readout applications.

On the other hand, $1/f$ noise of the CMOS transistors limits the power reduction and process induced transistor mismatches degrades the CMRR of the CBIA.

Table 2.1 Comparison of the three-opamp, switched-capacitor, and CBIA architectures for biopotential readout applications

	Three-Opamp IA	SC IA	CBIA
Low Power Dissipation	x	x	✓
Free of Noise Fold-Over	✓	x	✓
High Input Impedance	✓	x	✓
CMRR Independent from Matching of Passives	x	x	✓
CMRR Independent from Matching of Transistors	x	x	x
Negligible $1/f$ Noise in the Signal Bandwidth	x	x	x

The chopper modulation technique [29] can be used both for increasing the CMRR of the amplifiers and for eliminating the $1/f$ noise of the CMOS transistors (See Sect. 2.5 for further description of the chopper modulation technique). However, the main disadvantage of the chopper modulated amplifiers is the inherent DC coupling. Thus, they also amplify the differential DC electrode offset voltage between the biopotential electrodes. References [34–36] addresses the AC coupling issue in IAs using the chopper modulation technique. Reference [34] uses off-chip HPFs for filtering the electrode offset voltage. However, this technique not only results in large number of off-chip components for multi-channel biopotential readout front-ends, but also implements a very low input-impedance amplifier and degrades the signal-to-noise ratio of the IA. Reference [35] uses a differential difference amplifier for introducing HPF characteristics to a chopper modulated IA. However, this technique consumes excessive power due to the resistive feedback topology. Finally, Ref. [36] implements a low-power chopper stabilized IA with monolithic HPF. Although, the circuit achieves 105 dB CMRR and eliminates majority of the $1/f$ noise, the input impedance of the amplifier is very low ($7.5 \text{ M}\Omega$) especially for EEG acquisition systems, where a minimum of $100 \text{ M}\Omega$ is required [37].

2.5 Introduction to Chopper Modulation Technique

The operation principle of the chopper modulation technique is described in Fig. 2.5 [38]. The low frequency input signal (the bandwidth of the signal must be smaller than $f_{chop}/2$ to prevent aliasing) is modulated with the square wave modulation signal, $m(t)$. This shifts the frequency spectrum of the input signal, $X(s)$, to the odd harmonics of f_{chop} . Then, the modulated input signal is amplified by the amplifier with transfer function $A(f)$, and demodulated with $m(t)$. This shifts the modulated spectrum back to its original location, leaving replicas at the odd harmonics of f_{chop} . These replicas can be filtered by a LPF.

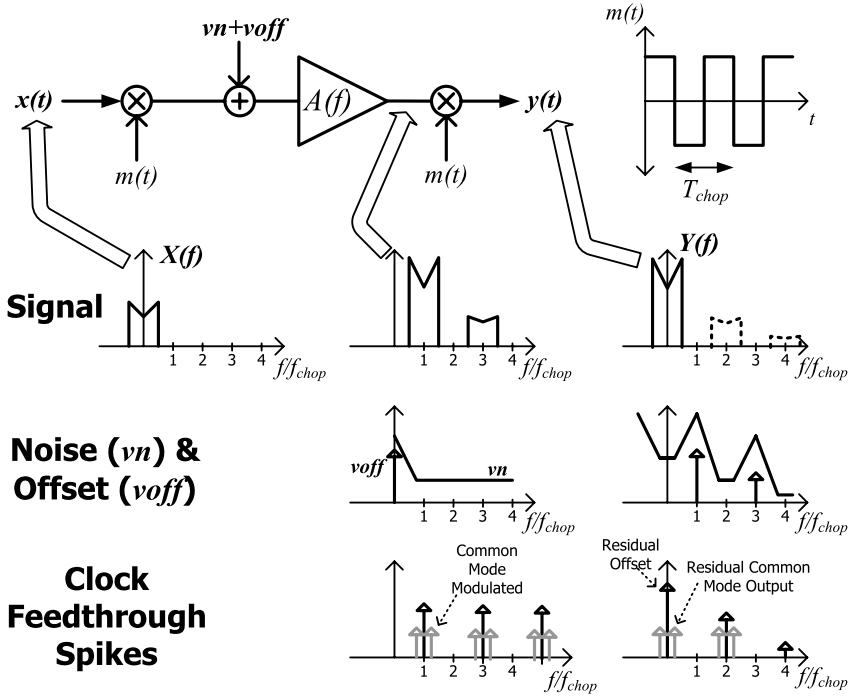


Fig. 2.5 Operation principle of chopper modulation technique. Input signal is modulated by $m(t)$, amplified by $A(f)$, and demodulated by $m(t)$

Subsections 2.5.1 and 2.5.2 will present the necessary formulas for understanding the operation of the chopper modulation technique. More detailed analysis of the chopper modulated amplifiers can be found in [29, 39–41].

2.5.1 Noise Analysis of Chopper Modulation Technique

Figure 2.5 describes the principle of how the chopper modulation technique eliminates the $1/f$ noise of the MOS transistors. The output noise and the offset of the core amplifier are indicated by v_n and v_{off} , which are only modulated by the output modulator. Therefore, the input referred noise of a chopper modulated amplifier is equivalent to v_n , multiplied with a square wave with frequency f_{chop} , when referred to the input of the chopper modulated amplifier. Hence, the double-sided input-referred voltage noise power spectral density (PSD), $S_{in}(f)$, of the amplifier can be written as:

$$S_{in}(f) = \left(\frac{2}{\pi}\right)^2 \sum_{n=-\infty, odd}^{\infty} \frac{1}{n^2} S_{vn}(f - n f_{chop}) \quad (2.6)$$

This equation should be handled separately for the thermal noise and the $1/f$ noise. Considering first the thermal noise component, (2.6) can be approximated as (2.7), if the f_c of the amplifier is much larger than f_{chop} [29]. This equation is only valid for the region where $|f| < 0.5f_{chop}$. Further approximation reduces (2.7) to (2.8) considering that $f_c \gg f_{chop}$:

$$S_{in,thermal}(f) \cong S_{in,thermal}(f=0) = S_0 \left[1 - \frac{\tanh(\frac{\pi}{2} \frac{f_c}{f_{chop}})}{\frac{\pi}{2} \frac{f_c}{f_{chop}}} \right] \quad (2.7)$$

$$S_{in,thermal} \cong S_0 \quad \text{for} \quad \left| \frac{f}{f_{chop}} \right| \leq 0.5 \text{ and } \frac{f_c}{f_{chop}} \gg 1 \quad (2.8)$$

As a result, the thermal noise of the chopper modulated amplifiers is not affected from the chopping operation as long as f_c of the amplifier is much larger than f_{chop} , which is due to the fact that the chopping operation only periodically changes the sign of the thermal noise.

On the other hand, considering that the $1/f$ noise of an amplifier is in the form of (2.9), the PSD of the input referred $1/f$ noise can be approximated by inserting (2.9) to (2.6), which can be expressed as (2.10) and indicates that the input referred $1/f$ noise of chopper modulated amplifiers can be approximated by a white noise component in the baseband [29].

$$S_{1/f}(f) = S_0 \frac{f_{c,1/f}}{|f|} \quad (2.9)$$

$$S_{in,1/f}(f) \cong 0.8525 S_0 \frac{f_{c,1/f}}{f_{chop}} \quad (2.10)$$

As a result, the total input referred noise of the amplifier in the baseband can be calculated by combining (2.8) and (2.10) as:

$$S_{in,total}(f) \cong S_0 \left(1 + 0.8525 \frac{f_{c,1/f}}{f_{chop}} \right) \quad \text{for} \quad \left| \frac{f}{f_{chop}} \right| \leq 0.5 \text{ and } \frac{f_c}{f_{chop}} \gg 1 \quad (2.11)$$

As a conclusion, the chopper modulation technique can effectively eliminate the $1/f$ noise of the MOS transistors without affecting the thermal noise, if f_{chop} can be selected to be much higher than $f_{c,1/f}$.

2.5.2 Charge Injection and Residual Offset of Chopper Modulated Amplifiers

Theoretically chopping amplifiers can achieve zero input referred offset voltage, since the offset of the core amplifier is modulated by the output chopper and can

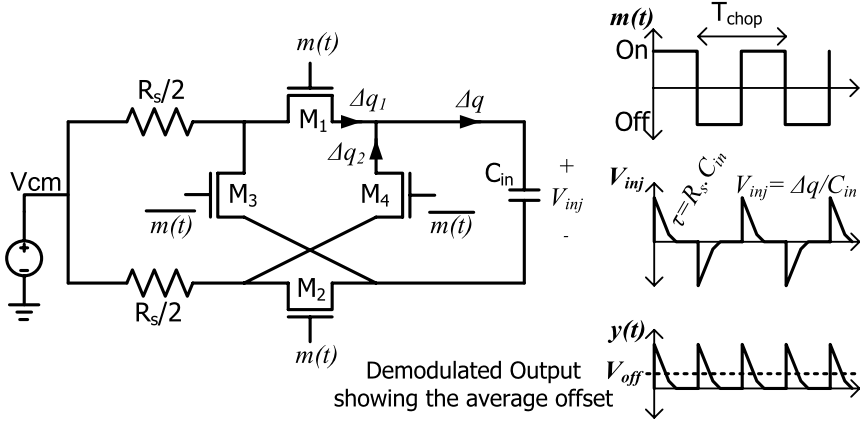


Fig. 2.6 Input modulator schematic of a chopper amplifier describing the charge injection from the nMOS switches to the input of the amplifier

be filtered. However, due to the non-ideality of the chopper switches, a residual offset remains. Figure 2.6 shows the schematic of a chopper modulator implemented with nMOS switches. Switches M_1 , M_2 and M_3 , M_4 are periodically toggled by the modulator signals $m(t)$ and $\bar{m}(t)$, respectively. During the switching of the nMOS transistors a certain amount of charge is injected to the source and drain of the MOS switch [42]. Although, in an ideal situation the charge injection of the transistors M_1 and M_2 are equal and appears as common-mode at the input of the amplifier, there is always a small mismatch, Δq_1 , which is injected to the input capacitance of the amplifier, C_{in} . Similarly, the mismatch between M_3 and M_4 results in an equivalent charge injection of Δq_2 . As a result, the total equivalent charge that is injected to the input of the amplifier can be written as:

$$\Delta q = |\Delta q_1 - \Delta q_2| \quad (2.12)$$

which results in an equivalent differential input voltage of:

$$V_{inj} = \frac{\Delta q}{C_{in}} \quad (2.13)$$

at the input of the amplifier with time constant:

$$\tau_{inj} = R_s C_{in} \quad (2.14)$$

as illustrated in Fig. 2.6. The input voltage, V_{inj} is amplified by the amplifier and then demodulated by the output chopper demodulator, creating an error output voltage, which has an average DC level of V_{off} . Assuming an amplifier with infinitely large bandwidth. The total input referred offset of the amplifier can be written as [40]:

$$V_{off} = 2\tau \cdot f_{chop} \cdot V_{inj} \quad (2.15)$$

As a conclusion, the offset of the chopper modulated amplifiers depend on the source resistance and the amount of the charge injection to the input. On the other hand, it is independent of the input capacitance of the amplifier. Assuming that the source resistance is defined by the sensor, where the readout is connected to, the offset of the chopped amplifiers can be decreased by reducing the sizes of the chopper switches or decreasing the chopping frequency. More detailed analysis about the offset in chopper amplifiers can be found in [39–41].

Several techniques have been proposed in the literature for reducing the inherent DC offset problem of the chopper modulated amplifiers. Reference [38] uses a bandpass filter between the input and the output choppers. However, matching of the bandpass filter center frequency with the chopping frequency limits the efficiency of this technique. Reference [43] uses nested choppers, where in addition to the input and output modulators, another pair of slow chopping modulators are used to modulate the output spikes of the fast modulator. Although, this technique can be very efficient for slow signals, biopotential signals have too large bandwidth for this solution (1 kHz bandwidth is necessary for EMG signals). Another technique is proposed by [44]. It uses a SC notch filter with synchronous integration after the output modulator to filter both the chopping ripple and the modulated amplifier offset, however results in excess quiescent current and complexity in the signal path.

2.5.3 Signal Distortion in Chopper Modulated Amplifiers

Signal distortion problem appears in chopper amplifiers due to the finite bandwidth of the core amplifier. Figure 2.7 describes the signal distortion in chopper modulated amplifiers. The differential input signal is modulated with the square wave modulation signal. However, due to the finite bandwidth of the core amplifier, high frequency components of the square wave is filtered by the core amplifier. When

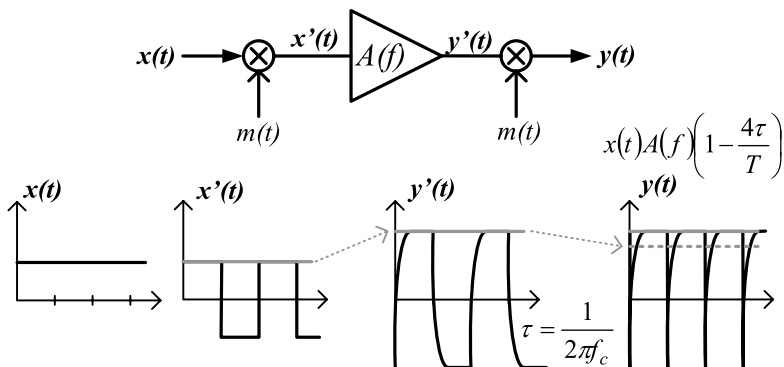


Fig. 2.7 Signal distortion problem in a chopper modulated amplifier due to the finite bandwidth of the core amplifier

this signal is demodulated by the output chopper, signal distortion in the shape of spikes appears at the output with the time constant:

$$\tau = \frac{1}{2\pi f_c} \quad (2.16)$$

The main consequence of these spikes is the reduction in the gain of the chopper modulated amplifier, which can be derived by considering a DC input voltage and calculating the average value of the output voltage for half the period of the chopping signal:

$$A_{chopped}(f) = A(f) \left(1 - \frac{4\tau}{T} \right) \quad (2.17)$$

It should be noted that the techniques presented in the Sect. 2.5.2 are also effective for reducing the signal distortion in chopper modulated amplifiers.

2.5.4 CMRR of the Chopper Modulated Amplifiers

Basically, there are two different mechanisms that define the CMRR of the conventional amplifiers: *Systemic common-mode gain*, which is due to the topology of the IA and *mismatch induced common-mode gain*, which is due to the process induced mismatches. Both of these CMRR reduction mechanisms can be eliminated by the chopper modulation technique.

The chopper structure shown in Fig. 2.6 is transparent to common-mode signals. Therefore, the input common-mode signal passes through the input chopper without being modulated and appears as a common-mode input to the core amplifier. The common-mode gain of the core amplifier converts the common-mode input into differential output. However, this differential output voltage, which is due to the non-zero common-mode gain of the amplifier, is modulated by the output modulator. Thus, it can be eliminated in a similar way the 1/f noise and the offset of the IA are filtered.

2.6 Conclusions

Biopotential readout circuits suffer from various problems for extracting biopotential signals. The extremely weak amplitudes of the biopotential signals make them susceptible to various correlating signals. Table 2.2 summarizes the requirements of a configurable readout front-end for biopotential acquisition systems.

The first problem is the 1/f noise of the CMOS transistors that dominates the noise of the readout circuit in the frequency band of the biopotential signals. Moreover, there is the interference from the mains, thus the readout circuit must achieve high CMRR to reject the large common-mode signals, while amplifying the biopotential signals. Both the interference and the 1/f noise problem can be solved by

Table 2.2 Requirements of a configurable readout front-end for biopotential acquisition systems

Problem	Solution	Technique
1/f Noise	1/f noise Filtering	Chopper Modulation
Common-Mode Interference	High CMRR	Chopper Modulation
Differential DC Electrode Offset	HPF Characteristics	?
Configurability for Different Biopotential Signals	Variable Gain	SC
		Resistive
		?
	Variable Bandwidth	?
Long Term Power Autonomy	Low-Power Design	?

using the chopper modulation technique. However, there is the problem of the differential DC offset between the electrodes. This DC voltage is orders of magnitude larger than the biopotential signals and can saturate the IA. Thus, the IA must have HPF characteristics for filtering the differential DC electrode offset voltage. Unfortunately, the chopper amplifiers are inherently DC coupled.

Therefore, there is a need for a chopper modulated IA with HPF characteristics, so that the 1/f noise, the interference, and the differential DC offset problems can be solved and high quality biopotential signals can be extracted. In addition, configurable characteristics for different biopotential signals and ultra low power dissipation for long term power autonomy is a must for portable biopotential acquisition systems.

Biopotential Readout Circuits for Portable Acquisition
Systems

Yazicioglu, R.F.; van Hoof, C.; Puers, R.

2009, XV, 164 p., Hardcover

ISBN: 978-1-4020-9092-9